ON THE FORM OF THE *SPITZER* LEAVITT LAW AND ITS DEPENDENCE ON METALLICITY

D. MAJAESS[1], D. G. TURNER[1], AND W. GIEREN[2]
[1] Department of Astronomy & Physics, Saint Mary's University, Halifax, NS B3H 3C3, Canada; dmajaess@ap.smu.ca
[2] Departamento de Astronomía, Universidad de Concepción, Casilla 160-C, Concepción, Chile

ABSTRACT

The form and metallicity dependence of *Spitzer* mid-infrared Cepheid relations are a source of debate. Consequently, *Spitzer* 3.6 and 4.5 μm period–magnitude and period–color diagrams were re-examined via robust routines, thus providing an alternative interpretation to consider. The relations (nearly mean-magnitude) appear non-linear over an extensive baseline ($0.45 < \log P_0 < 2.0$), particularly the period–color trend, which to first order follows constant (3.6–4.5) color for shorter-period Cepheids and may transition into a bluer convex trough at longer periods. The period–magnitude functions can be described by polynomials (e.g., $[3.6\,\mu\text{m}] = K_0 - (3.071 \pm 0.059)\log P_0 - (0.120 \pm 0.032)\log P_0{}^2$), and Cepheid distances computed using 3.6 and 4.5 μm relations agree with each other and the latter provides a first-order consistency check (CO sampled at 4.5 μm does not seriously compromise those distances). The period–magnitude relations appear relatively insensitive to metallicity variations ([Fe/H] $\sim$ 0 to -0.75 $|\gamma| < 0.1$ mag dex^{-1}), a conclusion inferred partly from comparing galaxy distances established from those relations and NED-D ($n > 700$), yet a solid conclusion awaits comprehensive mid-infrared observations for metal-poor Cepheids in IC 1613 ([Fe/H] ~ -1). The Cepheid-based distances were corrected for dust obscuration using a new ratio (i.e., $A_{3.6}/E_{B-V} = 0.18 \pm 0.06$) deduced from GLIMPSE (*Spitzer*) data.

Key word: stars: variables: Cepheids

Online-only material: color figures

1. INTRODUCTION

Spitzer mid-infrared observations of Cepheid variables have been employed to constrain stellar mass loss and anchor the cosmic distance scale (e.g., Neilson et al. 2009; Monson et al. 2012). Regarding the latter, the principal aim is to establish firmer constraints on the Hubble constant and cosmological models (Freedman et al. 2011). However, ambiguities linger concerning the form and metallicity dependence of mid-infrared Cepheid relations.

The impetus for obtaining *Spitzer* observations stems partly[3] from the diminished impact of dust extinction on infrared-based distances ($A_{3.6}/A_V \sim 0.06$, Section 2.4). Crucially, uncertainties tied to neglecting variations in the extinction law are reduced. The extinction law varies throughout the Galaxy, and a 20% uncertainty ($\sigma_{R_V}/R_V \sim 0.2$) merely contributes $\sigma_{\mu_0} \sim 0\overset{\text{m}}{.}01$ to the mid-infrared distance modulus (assuming $E_{B-V} = 0.10 \pm 0.03$). Conversely, variations in the extinction law can significantly impact Cepheid and star cluster distances that rely solely on shorter-wavelength data (e.g., Turner 2012a; Carraro et al. 2013 and discussion therein).

The aforementioned points reiterate the importance of *Spitzer* observations. However, a partial account provided below highlights the diverse opinions expressed concerning the form and metallicity dependence of mid-infrared Cepheid relations. Ngeow & Kanbur (2008), Madore et al. (2009), and Marengo et al. (2010) cited different slopes for linear *Spitzer* period–magnitude relations, while Neilson et al. (2009) suggested that function is non-linear (see also Ngeow & Kanbur 2010). For example, Ngeow & Kanbur (2008) obtained $\alpha = -3.26$ for the slope of the 3.6 μm relation using the OGLE[4]

and SAGE[5] data sets ($0.5 < \log P < 1.7$), whereas Madore et al. (2009) favored a steeper slope inferred by correlating the Persson et al. (2004) and SAGE catalogs ($\log P > 0.8$). A shallower slope may arise partly from the inclusion of shorter-period Cepheids that could suffer increased photometric contamination, particularly for distant targets (e.g., Macri et al. 2006; Madore et al. 2009; Majaess et al. 2013). However, Ngeow & Kanbur (2010) deduced analogous period–magnitude relations for relatively nearby Cepheids in the Small Magellanic Cloud (SMC) that occupy low- and high-density regions.

Marengo et al. (2010) and Ngeow et al. (2012b) found certain models produced *Spitzer* period–magnitude and period–color relations that did not match observations spanning an extended abundance baseline (see also Ngeow et al. 2012a and discussions therein). Observations imply that the same slope characterizes 3.6 and 4.5 μm period–magnitude relations for SMC and LMC Cepheids (Ngeow & Kanbur 2010), which exhibit mean abundances of [Fe/H] $\sim -0.75, -0.33$ accordingly (Luck et al. 1998; Mottini et al. 2006). Marengo et al. (2010) attempted to extend the baseline to include Galactic Cepheids ([Fe/H] ~ 0), but the effort was marred by inconsistencies associated with the available calibrating data (see also Ngeow & Kanbur 2010 and discussions therein). Hackwell & Gehrz (1974) and Marengo et al. (2010) noted that the 4.5 μm passband samples CO absorption features, which presumably alter the *Spitzer* Cepheid relations and introduce a metallicity effect. Scowcroft et al. (2011) confirmed the former finding by demonstrating that cooler long-period Cepheids exhibit colors that are modulated by the absorption and disassociation of CO, whereas their hotter short-period counterparts are less affected since the molecule is gradually disassociated. Freedman & Madore (2011) estimated that 3.6

---

[3] See Freedman et al. (2011, their Section 2).
[4] Optical Gravitational Lensing Experiment (e.g., Soszyński et al. 2008, 2010).

[5] Surveying the Agents of a Galaxy's Evolution (Meixner et al. 2006; Gordon et al. 2011).

and 4.5 μm Cepheid data exhibit a metallicity dependence of $\gamma = -0.39 \pm 0.16$ and -0.25 ± 0.18 mag dex^{-1}, respectively. The former estimate was revised by Freedman et al. (2011) to $\gamma = -0.09 \pm 0.29$ mag dex^{-1}. Those results are tied partly to published abundance estimates for individual LMC Cepheids, yet it is unclear whether systematic effects pervade such individual determinations,[6] although a mean metallicity derived from an entire sample appears reliable (Luck et al. 1998; Romaniello et al. 2008).

In this study, the form and metallicity dependence of *Spitzer* period–magnitude and period–color relations are reinvestigated. The relation linking the total extinction at 3.6 μm ($A_{3.6}$) to the optical color excess (E_{B-V}) is likewise derived from *Spitzer* data, as the correlation is necessary for computing Cepheid distances using the period–magnitude relations derived.

2. ANALYSIS

2.1. 3.6 and 4.5 μm Period–Magnitude Relations

3.6 and 4.5 μm period–magnitude relations are now inferred from LMC and SMC Cepheids. The LMC sample was assembled by correlating HV[7] Cepheids tabulated by Madore (1985) and Persson et al. (2004) with SAGE (*Spitzer*) photometry (a mean of random-phase data). Fundamental-mode Cepheids cataloged by OGLE were likewise added to the sample. For the SMC analysis, the Madore (1985) and OGLE catalogs were paired with SAGE photometry. A period cutoff of $\log P_0 > 0.45$ was imposed to mitigate biases stemming from a reputed change in slope near $\log P \sim 0.4$ (Ngeow & Kanbur 2010), to ensure magnitude uncertainties were satisfactory, to reduce the effects of photometric contamination, and to ensure that brighter Cepheids on the blue edge of the instability strip were not preferentially sampled (Sandage 1988; see also Appendix A in Freedman et al. 2001). The $\log P < 2.0$ limit was adopted to avoid the inclusion of Leavitt variables (Grieve et al. 1985), which may adhere to a separate slope (Persson et al. 2004, their Figure 3).

The nearly mean-magnitude period–color (3.6–4.5) relation examined in Section 2.3 is characterized by a higher-order polynomial over the baseline examined, thus hinting that the period–magnitude relations are non-linear. A single linear period–magnitude function does not adequately describe both the short- and long-period domains (see also Neilson et al. 2009). Longer-period Cepheids ($\log P > 1.45$) displayed a $\Delta[3.6\,\mu m] \gtrsim 0\overset{m}{.}06$ offset relative to a linear fit, whereby the latter fit yields values systematically too faint. Longer-period Cepheids are important granted the stars are preferentially sampled within remote galaxies in the Hubble flow. Efforts toward achieving precision cosmology ($\sigma_{H_0}/H_0 < 3\%$) hinge on reducing sources of uncertainty for such stars, especially since certain Cepheid-based determinations of H_0 exhibit tension with the new Planck results (Planck Collaboration et al. 2013; see also Freedman et al. 2012; Tammann & Reindl 2012 and discussions therein).

Robust fitting routines were employed since the method of least squares is acutely sensitive to outliers,[8] whereas the former techniques are less affected by spurious data and more apt to identify the underlying trend. The robust routine applied seeks to minimize the sum of the absolute deviations, rather than the sum of the squared deviations. The routine was used in concert with a 4σ clip, twice iterated. That conservative procedure was followed because Madore et al. (2009) suggested that differences between the various determinations for the period–magnitude relation may arise partly from aggressive clipping/iterations.

The following functional forms were deduced and characterized LMC Cepheids across an extensive baseline ($0.45 < \log P_0 < 2.0$):

$$[3.6\,\mu m] = (15.917 \pm 0.026) - (3.077 \pm 0.064)\log P_0$$
$$- (0.114 \pm 0.036)\log P_0{}^2,$$
$$[4.5\,\mu m] = (15.890 \pm 0.026) - (3.084 \pm 0.065)\log P_0$$
$$- (0.082 \pm 0.036)\log P_0{}^2. \tag{1}$$

For SMC Cepheids the corresponding relations are

$$[3.6\,\mu m] = (16.411 \pm 0.063) - (3.041 \pm 0.143)\log P_0$$
$$- (0.145 \pm 0.074)\log P_0{}^2,$$
$$[4.5\,\mu m] = (16.382 \pm 0.061) - (3.076 \pm 0.140)\log P_0$$
$$- (0.104 \pm 0.072)\log P_0{}^2. \tag{2}$$

The magnitude of the squared term increases slightly if longer-period Cepheids are given more weight, and the uncertainties subsequently diminish. Yet a single quadratic expression is preferred over two linear relations since the statistical weight of the entire Cepheid demographic can be exploited to reduce uncertainties. Relatively nearby short-period Cepheids detected in the Magellanic Clouds outnumber their long-period counterparts, as low-mass metal-poor stars cross the instability strip with an extended blue loop (Becker 1985). The initial mass function implies that low-mass objects are more numerous, which in concert with the aforementioned trend explains the shift in the distribution of Magellanic Cloud Cepheids toward shorter periods.[9]

2.2. Metallicity Effects at 3.6 and 4.6 μm

The coefficients tied to the pulsation period in Equations (1) and (2) agree to within the uncertainties. Thus the slopes for the 3.6 and 4.5 μm period–magnitude relations are comparatively insensitive to metallicity variations from [Fe/H] ~ -0.33 to -0.75 (see also Ngeow & Kanbur 2010). The 3.6 and 4.5 μm zero points and coefficients for a given Magellanic Cloud agree to within the uncertainties, thus indicating that distances established from the latter passband can serve as a first-order consistency check (CO is sampled in the 4.5 μm passband, e.g., Hackwell & Gehrz 1974).

The impact of metallicity can likewise be assessed by comparing NED-D[10] and *Spitzer*-based Cepheid distances. Relative offsets between the SMC/LMC, and the SMC/Milky Way, are now evaluated. The latter comparison provides a desirably

---

[6] The Freedman & Madore (2011) analysis, which relies on published abundance estimates found in the literature for individual Cepheids, implies that the BV Wesenheit function displays a nearly negligible dependence on metallicity, whereas certain researchers suggest otherwise (Tammann et al. 2003; Majaess et al. 2009; Bono et al. 2010; see also the discussion in Freedman & Madore 2011 concerning the VI_c Wesenheit function).
[7] Harvard Variable.

[8] Certain outliers may be Cepheids exhibiting high mass loss (Neilson et al. 2009).
[9] There exists a period–mass–luminosity relation (e.g., Turner 2012b).
[10] NASA/IPAC Extragalactic Database Master List of Galaxy Distances (Steer & Madore 2011).

large abundance baseline (Δ[Fe/H] ~ -0.75). Cepheid distances were calculated via the following relations derived from a weighted mean of Equations (1) and (2):

$$[3.6\,\mu\text{m}] = K_0 - (3.071 \pm 0.059)\log P_0$$
$$- (0.120 \pm 0.032)\log P_0^2,$$
$$[4.5\,\mu\text{m}] = K_0 - (3.083 \pm 0.059)\log P_0$$
$$- (0.086 \pm 0.032)\log P_0^2. \qquad (3)$$

The offset between Cepheids in the SMC/LMC is $\Delta K_{0,3.6} = 0.501 \pm 0.068$, while the differential for the SMC/Galaxy is $\Delta K_{0,3.6} = 18.938 \pm 0.077$. Marginal extinction corrections were applied to the Cepheid distances (Section 2.4), and the Galactic calibration used is discussed below. The corresponding 4.5 μm results are $\Delta K_{0,4.5} = 0.480 \pm 0.066$ and 18.921 ± 0.075, respectively. The values compare favorably to means tabulated from NED-D data ($n > 700$), namely $\Delta K_0 = 0.450 \pm 0.012$ and 18.930 ± 0.011. The results imply values of $\gamma_{3.6} \sim -0.10 \pm 0.10, -0.01 \pm 0.06$ and $\gamma_{4.5} \sim -0.06 \pm 0.10, 0.01 \pm 0.06$ mag dex^{-1}. The associated uncertainties underscore the need for continued research, and formal uncertainties cited throughout the analysis may underestimate the true uncertainties.

In sum, the analyses imply that distances inferred from the 3.6 and 4.5 μm period–magnitude relations are relatively insensitive to variations in metallicity ([Fe/H] ~ 0 to -0.75). However, a comparison including IC 1613 is required since Cepheids in that galaxy ([Fe/H] ~ -1) are more metal-poor than their SMC counterparts. Reliable *Spitzer* data are merely readily available for five $\log P < 2$ Cepheids in IC 1613 (Freedman et al. 2009), and a comparison at present may be premature given those small statistics, the potential for inadequate instability strip filling, and concerns regarding photometric contamination expressed in the literature (Freedman et al. 2009). Freedman et al. (2011, their Table 1) plan to obtain comprehensive mid-infrared observations for additional Cepheids in IC 1613.

The Galactic mid-infrared data were adopted verbatim from Monson et al. (2012), who presented complete light curves for numerous Galactic Cepheids. Monson et al. (2012) paired their new photometry with IRSB,[11] parallax, and cluster Cepheid data to establish a Galactic calibration (e.g., Benedict et al. 2007; Fouqué et al. 2007; Turner 2010). That calibration consists of Cepheids with near solar abundances ([Fe/H] ~ 0), and is hence important for assessing the impact of metallicity. However, the Galactic calibration may presently be the most difficult to construct, since the constituent Cepheids exhibit sizable differential reddening and do not lie at a common distance. The Galactic calibration currently suffers from a lack of solid long-period calibrators, and parameters for cluster Cepheids are being contested and revised (e.g., Anderson et al. 2012; Majaess et al. 2012). The IRSB parameters for long-period Cepheids rely directly on the *p*-factor, the form of which is actively debated given its importance (Gieren et al. 2005; Storm et al. 2011; Ngeow et al. 2012c; Neilson et al. 2012).[12] Nevertheless, the resulting non-linear fits (Equation (3)) to the Monson et al. (2012) data[13] yield $K_{0,3.6} = -2.545 \pm 0.045$

and $K_{0,4.5} = -2.551 \pm 0.043$. The results were derived by adopting the $\log P_0$ coefficient established from Magellanic Cloud Cepheids (Equation (3)), while permitting $\log P_0^2$ and K_0 to vary. The aim was to examine whether the resulting coefficients for $\log P_0^2$ match those determined for Magellanic Cloud Cepheids (Equation (3)). The results agree to first order, namely, -0.10 (3.6 μm) and -0.05 (4.5 μm). However, those determinations are merely suggestive owing to the lack of numerous solid long-period calibrators.

2.2.1. Comparison of the LMC Data

The Madore et al. (2009) LMC sample results from a correlation of the Persson et al. (2004) and SAGE catalogs (a mean of random-phase data), whereas Scowcroft et al. (2011) subsequently obtained complete mid-infrared light-curve coverage for the Cepheids as part of the Carnegie Hubble Project. Equation (3) is now applied to the LMC data of Madore et al. (2009) and Scowcroft et al. (2011). The period coefficients remained fixed, and the zero point was allowed to vary. Zero points of $K_{0,3.6} = 15.939 \pm 0.030$ and 15.911 ± 0.012 were derived accordingly. The results agree to within the formal uncertainties, and a visual inspection reveals a reliable fit (Figure 1). A least-squares solution was obtained since extreme outliers are absent.

The Scowcroft et al. (2011) data (warm *Spitzer*) are tied to a separate photometric reduction, whereas the Madore et al. (2009), Ngeow & Kanbur (2008), and Figure 1 samples rely on SAGE photometry. A comparison between the SAGE and Scowcroft et al. (2011, hereafter S11) 3.6 μm photometry reveals a color offset ($\Delta[3.6]_{\text{S11-SAGE}} \sim -0.9 \times (3.6\text{–}4.5)_{\text{SAGE}}$). The offset may stem from uncertainties in the photometric standardization, but additional research is ultimately needed to identify the source.

2.3. Period–Color Relation

Period–color data for LMC and SMC Cepheids were examined (Figure 1). The observations are characterized by a non-linear fit over the period baseline, whereby shorter-period Cepheids adhere to a near constant color and a convex trough may describe the longer-period domain.[14] Those trends can be explained in part by CO (see also Hackwell & Gehrz 1974; Marengo et al. 2010; Scowcroft et al. 2011; Monson et al. 2012). Figure 1 indicates that for shorter-period Cepheids the color is nearly constant as the temperature is sufficiently high to disassociate most CO. For longer-period (cooler) Cepheids CO absorption occurs, and the molecule is gradually disassociated in increasing amounts near the pulsation phase corresponding to temperature maximum. The period–color trend exhibits inflection points near $\log P \sim 0.75$, $\log P \sim 1.75$, and potentially $\log P > 2.2$. Additional analyses are warranted.

A mean color inferred from shorter-period Cepheids near the constant part of the trend yields $(3.6\text{–}4.5) = 0.023, 0.039$ for the LMC and SMC, respectively. The optical to mid-infrared color-excess ratio derived in Section 2.4 implies intrinsic colors of $(3.6\text{–}4.5)_0 = 0.015, 0.033$ (LMC/SMC). Galactic Cepheids (Monson et al. 2012) exhibit $(3.6\text{–}4.5)_0 = -0.022$, as deduced from a visual match to intermediate-period Cepheids in the LMC. That procedure was followed as the *Spitzer* Galactic sample does not presently contain numerous shorter-period

---

[11] Infrared Surface Brightness technique (Fouque & Gieren 1997).

[12] W. Gieren et al. (2013, in preparation) aim to constrain the *p*-factor using LMC Cepheids in double-lined eclipsing binary systems (Pietrzyński et al. 2010, 2011).

[13] The absolute magnitudes used were an averaged subset from IRSB, cluster Cepheid, and the Benedict et al. (2007) parallax results (see Monson et al. 2012).

---

[14] The period–color relation is nearly constant across the entire period baseline when sampled at the hottest pulsation phase (Monson et al. 2012, their Figure 9).
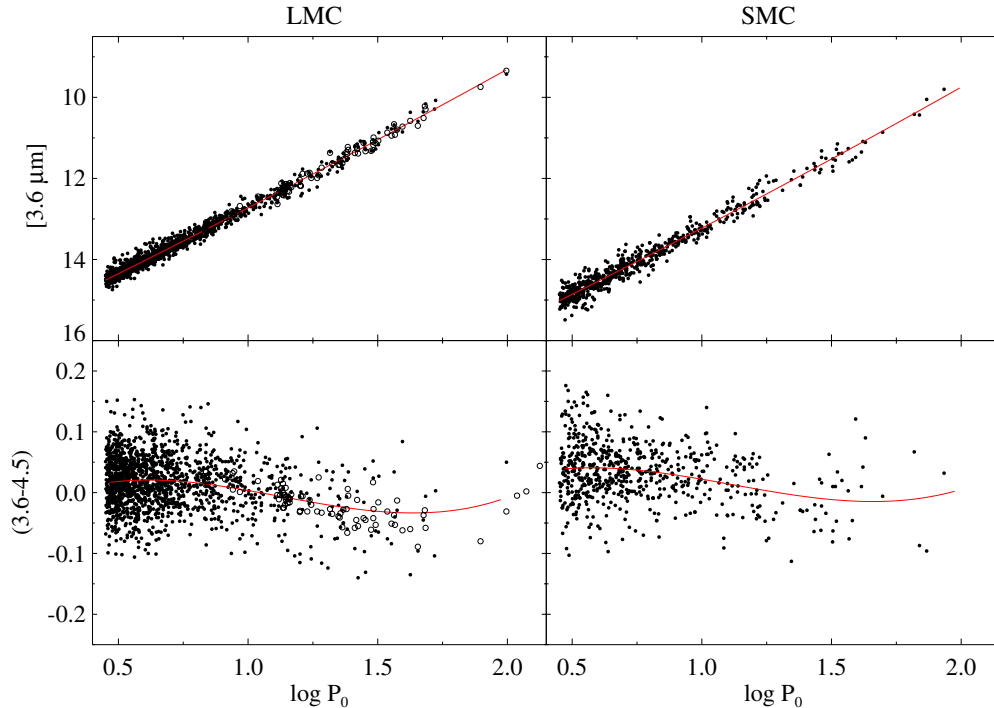
Figure 1. *Spitzer* period–magnitude and period–color diagrams for Cepheids in the Magellanic Clouds. The (nearly mean-magnitude) data are described by non-linear trends over an extended baseline ($0.45 < \log P_0 < 2.0$), particularly the period–color relation. Solid lines convey mean fits, and the data shown were cleaned of outliers via an iterative σ-clip. Filled circles represent SAGE photometry, while open circles are observations from Scowcroft et al. (2011).
(A color version of this figure is available in the online journal.)

Cepheids, and their longer-period counterparts can exhibit rather uncertain reddening estimates.[15]

Offsets between the intrinsic colors of the three galaxies are likely insignificant owing to uncertainties arising from photometric reductions and extinction corrections. Monson et al. (2012) note that the systematic error associated with *Spitzer* photometry for Galactic Cepheids may be $\sim 0\overset{m}{.}016$ in each passband (3.6 and 4.5 μm), and a similar uncertainty exists for the Magellanic Cloud photometry. More sizable photometric offsets can exist in optical surveys of star clusters (Stetson et al. 2004, their Table 3 for NGC 188) and the Magellanic Clouds (D. Majaess et al., in preparation). Alternatively, comprehensive mid-infrared observations of Cepheids in IC 1613 will dictate whether metallicity offsets the period–color relation ($\gamma_{3.6-4.5} \sim -0.07$ mag dex$^{-1} + ...$), as metal-poor Cepheids in IC 1613 are predicted to be intrinsically redder than their SMC, LMC, and Galactic counterparts (Monson et al. 2012, their Figure 10).

2.4. Extinction Law

Spitzer period–magnitude relations provide Cepheid distances once corrected for dust extinction. Most extragalactic Cepheids observed for the *Hubble Space Telescope* key project to measure H_0 are reddened by $E_{B-V} \sim 0.1$ (e.g., Figure 6 in Majaess 2010), and thus the resulting mid-infrared extinction is marginal. There are exceptions such as the Cepheids in NGC 6822 (Gieren et al. 2006) and Centaurus A (Ferrarese et al. 2007), that exhibit comparatively larger reddenings.

The ratios $A_{3.6}/E_{B-V}$ and $E_{3.6-4.5}/E_{B-V}$ are often used since E_{B-V} may be known a priori from other observations.

Those ratios are now derived from *Spitzer* (GLIMPSE[16]) data for O-type stars, which exhibit comparable intrinsic $(B - V)_0$ colors and sizable reddenings. O-type stars in the Skiff (2013) catalog were correlated with Two Micron All Sky Survey, *Spitzer*, and optical photometry. A linear relation between $(B - V)$ and $(3.6–4.5)$ is displayed in Figure 2, and defines $E_{3.6-4.5}/E_{B-V}$. A robust fit applied using an iterative σ-clip yielded $E_{3.6-4.5}/E_{B-V} = 0.06 \pm 0.01$.

To determine $A_{3.6}/E_{B-V}$, color ratios ($E_{3.6-\lambda}/E_{B-V}$) were plotted as a function of λ^{-1} and extrapolated to $\lambda \rightarrow \infty$. Intrinsic optical and near-infrared colors were adopted from Turner (1989 and references therein) and Straižys & Lazauskaitė (2009). Intrinsic mid-infrared colors were derived from the relevant color ratios (e.g., $(3.6 - J)$ versus $(B - V)$ was extrapolated to the mean $(B - V)_0$ adopted for an O-type star). Although O-type stars are advantageous given the reasons cited above, such young stars often occupy regions displaying polycyclic aromatic hydrocarbon emission, and thus the 8.0 and 5.8 μm data were bypassed to mitigate concerns regarding contamination. Figure 2 displays the extinction law diagram, whereby a polynomial fit to the data yields $A_{3.6}/E_{B-V} = 0.18 \pm 0.06$. The ratios derived are consistent with values adopted by Monson et al. (2012 and references therein).

Lastly, extinction laws vary throughout the Galaxy (e.g., Carraro et al. 2013; Nataf et al. 2013 and references therein), and appear anomalous for certain regions in the fourth Galactic quadrant sampled by GLIMPSE. However, altering the ratio to account for variations in the extinction law does not significantly impact estimated mid-infrared distances, hence a motivation for monitoring Cepheids with *Spitzer*. Applying the ratio derived

---

[15] D. Turner (in preparation) is reworking the Galactic cluster Cepheid calibration with the aim of improving intrinsic color and distance estimates.

[16] The Galactic Legacy Infrared Mid-Plane Survey Extraordinaire. GLIMPSE surveyed a portion of the fourth Galactic quadrant (Benjamin et al. 2003).
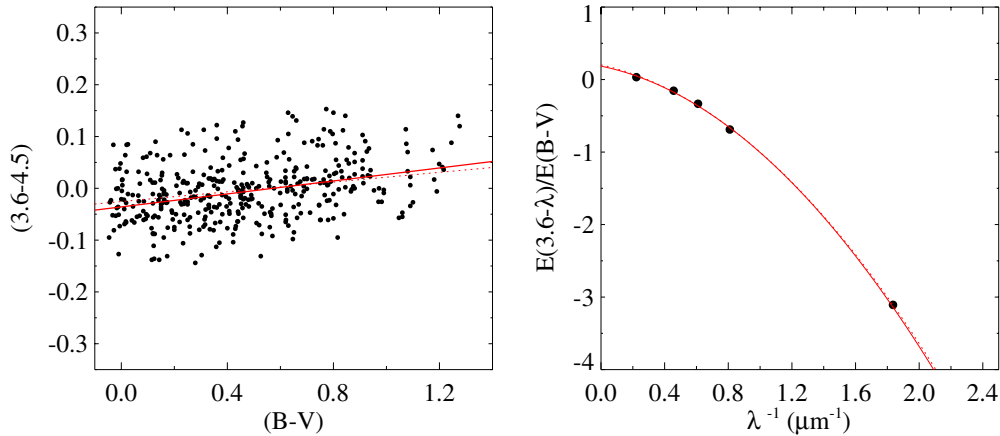
Figure 2. Left: a linear fit yields the ratio $E_{3.6-4.5}/E_{B-V} = 0.06 \pm 0.01$ (solid red line). Right: a polynomial fit to data including *Spitzer* (GLIMPSE) observations yields $A_{3.6}/E_{B-V} = 0.18 \pm 0.06$ (solid red line). The ratios are used to correct *Spitzer*-based Cepheid distances for dust extinction, thus stymieing the propagation of a systematic uncertainty into the distance scale. The dashed lines were inferred from parameters adopted by Monson et al. (2012 and references therein).

(A color version of this figure is available in the online journal.)

above to the mean LMC reddening ($E_{B-V} \sim 0.14$) yields $A_{3.6} \sim 0\overset{m}{.}025$.

2.5. Conclusions

Spitzer 3.6 and 4.5 μm period–magnitude and period–color relations (nearly mean-magnitude) were re-investigated (Figure 1). The LMC and SMC period–magnitude functions, and particularly the period–color trend, appear non-linear over an extended baseline ($0.45 < \log P_0 < 2.0$). Applying a quadratic period–magnitude function capitalizes on the statistical weight of short- and long-period Cepheids to improve certain distance determinations. Incidentally, Cepheid distances inferred from 3.6 and 4.5 μm data are consistent to first order, thus indicating that CO features present in the 4.5 μm passband do not seriously compromise the distances evaluated (the 4.5 μm distances can serve as a consistency check). The slope and zero point of the relations appear comparatively insensitive to metallicity variations ($[\mathrm{Fe/H}] \sim 0$ to -0.75, $|\gamma| < 0.1$ mag dex^{-1}). That was determined in part by comparing galaxy distances ($\Delta[\mathrm{Fe/H}] \sim -0.75$) inferred from the *Spitzer* period–magnitude relations and NED-D. The results support prior findings (Ngeow & Kanbur 2010; Freedman et al. 2011), yet a firm conclusion awaits a comparison between improved data for Cepheids in IC 1613 and the Milky Way. Further research is likewise required on models, as noted by Ngeow et al. (2012a), with the aim of reproducing the observed period–color trend (Figure 1). The latter is non-linear whereby (3.6–4.5) is nearly constant for shorter-period Cepheids, and the color may transition to a bluer convex trough at longer periods (Figure 1). Lastly, an extinction law ($A_{3.6}/E_{B-V} = 0.18 \pm 0.06$, Figure 2) was derived using *Spitzer* (GLIMPSE) observations in order to correct the distances for dust obscuration, and to avoid propagating a systematic uncertainty into the cosmic distance scale (and H_0).

REFERENCES

Anderson, R. I., Eyer, L., & Mowlavi, N. 2012, arXiv:1212.5119
Becker, S. 1985, in IAU Colloq. 82, Cepheids: Theory and Observation, ed. B. F. Madore (New York: Cambridge Univ. Press), 104
Benedict, G. F., McArthur, B. E., Feast, M. W., et al. 2007, AJ, 133, 1810
Benjamin, R. A., Churchwell, E., Babler, B. L., et al. 2003, PASP, 115, 953
Bono, G., Caputo, F., Marconi, M., & Musella, I. 2010, ApJ, 715, 277
Carraro, G., Turner, D., Majaess, D., & Baume, G. 2013, A&A, 555, A50
Ferrarese, L., Mould, J. R., Stetson, P. B., et al. 2007, ApJ, 654, 186
Fouqué, P., Arriagada, P., Storm, J., et al. 2007, A&A, 476, 73
Fouque, P., & Gieren, W. P. 1997, A&A, 320, 799
Freedman, W. L., & Madore, B. F. 2011, ApJ, 734, 46
Freedman, W. L., Madore, B. F., Gibson, B. K., et al. 2001, ApJ, 553, 47
Freedman, W. L., Madore, B. F., Scowcroft, V., et al. 2011, AJ, 142, 192
Freedman, W. L., Madore, B. F., Scowcroft, V., et al. 2012, ApJ, 758, 24
Freedman, W. L., Rigby, J., Madore, B. F., et al. 2009, ApJ, 695, 996
Gieren, W., Pietrzyński, G., Nalewajko, K., et al. 2006, ApJ, 647, 1056
Gieren, W., Storm, J., Barnes, T. G., III, et al. 2005, ApJ, 627, 224
Gordon, K. D., Meixner, M., Meade, M. R., et al. 2011, AJ, 142, 102
Grieve, G. R., Madore, B. F., & Welch, D. L. 1985, ApJ, 294, 513
Hackwell, J. A., & Gehrz, R. D. 1974, ApJ, 194, 49
Luck, R. E., Moffett, T. J., Barnes, T. G., III, & Gieren, W. P. 1998, AJ, 115, 605
Macri, L. M., Stanek, K. Z., Bersier, D., Greenhill, L. J., & Reid, M. J. 2006, ApJ, 652, 1133
Madore, B. F. 1985, in IAU Colloq. 82, Cepheids: Theory and Observation, ed. B. F. Madore (New York: Cambridge Univ. Press), 166
Madore, B. F., Freedman, W. L., Rigby, J., et al. 2009, ApJ, 695, 988
Majaess, D. 2010, AcA, 60, 55
Majaess, D., Turner, D., Gieren, W., Balam, D., & Lane, D. 2012, ApJL, 748, L9
Majaess, D., Turner, D., Gieren, W., Berdnikov, L., & Lane, D. 2013, Ap&SS, 344, 381
Majaess, D., Turner, D., & Lane, D. 2009, AcA, 59, 403
Marengo, M., Evans, N. R., Barmby, P., et al. 2010, ApJ, 709, 120
Meixner, M., Gordon, K. D., Indebetouw, R., et al. 2006, AJ, 132, 2268
Monson, A. J., Freedman, W. L., Madore, B. F., et al. 2012, ApJ, 759, 146
Mottini, M., Romaniello, M., Primas, F., et al. 2006, MmSAI, 77, 156
Nataf, D. M., Gould, A., Fouqué, P., et al. 2013, ApJ, 769, 88
Neilson, H. R., Nardetto, N., Ngeow, C.-C., Fouqué, P., & Storm, J. 2012, A&A, 541, A134
Neilson, H. R., Ngeow, C.-C., Kanbur, S. M., & Lester, J. B. 2009, ApJ, 692, 81
Ngeow, C., & Kanbur, S. M. 2008, ApJ, 679, 76
Ngeow, C.-C., & Kanbur, S. M. 2010, ApJ, 720, 626
Ngeow, C.-C., Kanbur, S. M., Bellinger, E. P., et al. 2012a, Ap&SS, 341, 105

Ngeow, C.-C., Marconi, M., Musella, I., Cignoni, M., & Kanbur, S. M. 2012b, ApJ, 745, 104
Ngeow, C.-C., Neilson, H. R., Nardetto, N., & Marengo, M. 2012c, A&A, 543, A55
Persson, S. E., Madore, B. F., Krzemiński, W., et al. 2004, AJ, 128, 2239
Pietrzyński, G., Thompson, I. B., Gieren, W., et al. 2010, Natur, 468, 542
Pietrzyński, G., Thompson, I. B., Graczyk, D., et al. 2011, ApJL, 742, L20
Planck Collaboration, Ade, P. A. R., Aghanim, N., et al. 2013, arXiv:1303.5076
Romaniello, M., Primas, F., Mottini, M., et al. 2008, A&A, 488, 731
Sandage, A. 1988, PASP, 100, 935
Scowcroft, V., Freedman, W. L., Madore, B. F., et al. 2011, ApJ, 743, 76
Skiff, B. A. 2013, VizieR Catalog: General Catalogue of Stellar Spectral Classifications
Soszyñski, I., Poleski, R., Udalski, A., et al. 2008, AcA, 58, 163

Soszyñski, I., Poleski, R., Udalski, A., et al. 2010, AcA, 60, 17
Steer, I., & Madore, B. 2011, NED-D: NASA/IPAC Extragalactic Database Master List of Galaxy Distances (http://ned.ipac.caltech.edu/Library/Distances/)
Stetson, P. B., McClure, R. D., & VandenBerg, D. A. 2004, PASP, 116, 1012
Storm, J., Gieren, W., Fouqué, P., et al. 2011, A&A, 534, A94
Straižys, V., & Lazauskaitė, R. 2009, BaltA, 18, 19
Tammann, G. A., & Reindl, B. 2012, Ap&SS, 341, 3
Tammann, G. A., Sandage, A., & Reindl, B. 2003, A&A, 404, 423
Turner, D. G. 1989, AJ, 98, 2300
Turner, D. G. 2010, Ap&SS, 326, 219
Turner, D. G. 2012a, Ap&SS, 337, 303
Turner, D. G. 2012b, JAVSO, 40, 502